

---

# Temporospatial Encoding of Acupuncture Effects in the Brain

# 2

Lijun Bai and Jie Tian

---

## 2.1 Introduction

Acupuncture is a traditional Chinese healing modality that has existed for more than 2500 years. In recent decades, acupuncture has gained popularity as an alternative and complementary therapeutic intervention in Western medicine (Hui et al. 2000). Acupuncture has been reported to be effective for the treatment of postoperative dental pain, chemotherapy-induced nausea and vomiting, carsickness and seasickness, and pregnancy-related nausea. Other research has demonstrated the promising utility of acupuncture as an adjunct or alternative treatment for drug addiction, stroke rehabilitation, asthma, headache (including tension headache and migraine), and chronic pain. Moreover, the National Institutes of Health (NIH) issued a consensus stating that acupuncture has fewer and less harmful side effects than pharmacological or surgical interventions, making acupuncture an attractive therapy for many indications.

Evidence from animal studies has demonstrated that acupuncture stimulation can facilitate the release of specific neuropeptides in the central nervous system (CNS) and elicit profound physiological and therapeutic effects (Han 2004; Xing et al. 2007). Studies of electroacupuncture (EA) in rats revealed that both low- and high-frequency stimulations could induce analgesia but their effects differ according to the types of endorphins released (Guo et al. 1996). Deep peripheral acupuncture stimulation has also been reported to activate various brain structures, including the limbic, hypothalamic, and brainstem nuclei (Pomeranz 2001).

---

L. Bai

The Key Laboratory of Biomedical Information Engineering, Ministry of Education,  
Department of Biomedical Engineering, School of Life Science and Technology,  
Xi'an Jiaotong University, Xi'an, China

J. Tian (✉)

CAS Key Laboratory of Molecular Imaging, Institute of Automation, Beijing, China  
e-mail: [jie.tian@ia.ac.cn](mailto:jie.tian@ia.ac.cn)

Although animal research clearly supports the role of specific neural pathways in the mechanisms of acupuncture effects, it is difficult to interpret these studies in the context of the more complex human experience, which includes expectation, emotion, and changes in cognition. With recent advancements in the resolution and sensitivity of the neuroimaging technologies such as positron emission tomography (PET), functional magnetic resonance imaging (fMRI), electroencephalography (EEG), and magnetoencephalography (MEG), it has become more feasible to assess and monitor the neurophysiological effects of acupuncture in the human brain. The wide range of physical effects exerted by acupuncture and its purported efficacy for a compendium of clinical pathologies suggest that the brain may be responsible for transmitting the needle stimulation into signals that restore or facilitate homeostatic balance within and across functional physiological systems (Mann 1992; Jeanette et al. 2000; Kaptschuk 2002; White et al. 2007).

With regard to the temporal effects of acupuncture, many studies have demonstrated that acupuncture can induce sustained effects in the brain even after the cessation of therapy (Bai et al. 2009a; Dhond et al. 2008; Price et al. 1984; Qin et al. 2008, 2011). These studies indicate the existence of time-variant features of acupuncture effects in wide brain networks (Bai et al. 2009b, c; Qin et al. 2011).

---

## 2.2 Methods of Analysis for Human Acupuncture Neuroimaging Studies

### 2.2.1 General Linear Model (GLM) Analysis

Voxel-wise application of a GLM is a standard way to analyze BOLD signal changes in response to a stimulus (e.g., acupuncture).

The GLM is a statistical linear model described by the following equation:

$$Y_i = X_i' \beta + \varepsilon_i \quad (2.1)$$

For the analysis of fMRI data, the given data  $Y_i$  at time index  $i$  is

$$Y_i = x_{i1}\beta_{i1} + \cdots + x_{ik}\beta_{ik} + x_{i,k+1}\beta_{i,k+1} + \cdots + x_{im}\beta_{im} + \varepsilon_i = x_i' \beta + \varepsilon_i \quad (2.2)$$

where  $x_{i1}, \dots, x_{ik}$  is the combined effect of  $k$  for different stimulus types in scan  $i$  and is often assumed to be additive but with different coefficients  $\beta_{i1}, \dots, \beta_{ik}$  that vary from voxel to voxel.

The combined fMRI response is modeled linearly as  $x_{i1}\beta_{i1} + \cdots + x_{ik}\beta_{ik}$ . The extra “responses”  $x_{i,k+1}, \dots, x_{im}$  at time  $i$  show the considerable drift over time of some voxels in fMRI time series data. Accordingly,  $x_{i,k+1}\beta_{i,k+1} + \cdots + x_{im}\beta_{im}$  describes the drift.  $\varepsilon_i$  is the random error.

The GLM aims to test whether the dynamic characteristics of neural responses in specific brain regions relate with some known input function (e.g., experimental design convoluted with hemodynamic function). GLM has arguably become the most widely used method for analyzing fMRI data and has proven particularly powerful for the analysis of event-related designs, given that a sequence of sparse events

occurring at random intervals affords a relatively specific predicted response, and good fit is often interpreted in terms of signal evoked by a particular psychological event (Worsley and Friston 1995; Wager et al. 2005). However, when the precise timing and duration of psychological events cannot be specified using a priori defined regressors that model predicted responses to psychological events of interest, the GLM becomes impractical (Lindquist et al. 2007).

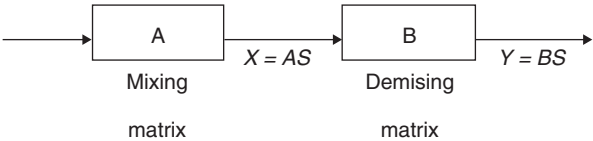
### 2.2.2 Independent Component Analysis (ICA)

The ICA transforms multivariate random signal into signal with multiple statistically independent components. ICA models have traditionally been used to perform blind separation, feature extraction, and signal detection, resulting in the development of many batch and adaptive algorithms. The ICA does not require a priori knowledge or specific assumptions about the time courses of processes contributing to the measured signals. In addition, ICA appears to have a broad developing prospect in the analysis of fMRI data from healthy and clinical populations, especially in the context of unpredictable transient patterns of brain activity associated with psychomotor task performance. A schematic diagram of ICA is shown in Fig. 2.1, where  $X$  is the result of multisource signals multiplied by mixing matrix  $A$ ,  $X=AS$ . We can obtain the solution of mixing matrix  $B$  when  $S$  and  $A$  are unknown, resulting in  $Y=BS$  as the optimal approximation of  $S$ .

Given the central limit theorem, the sum of independent random variables tends to follow a Gaussian distribution. Accordingly, the sum of independent random variables should be closer to the Gaussian distribution than any one variable involved. As a consequence, the combination yields the maximization of non-Gaussianity, such that the random variables most remarkably deviating from the Gaussian distribution can be regarded as one independent component of  $X$ . This method is called the non-Gaussian maximization method. In addition, there are many other methods used to estimate the ICA, such as approaches to estimate the mutual information minimum and maximum based on the information theory. Many ICA algorithms have been derived from this, such as maximizing or minimizing some related cost function, the adaptive algorithm based on a stochastic gradient, the widely used FastICA algorithm, and the Infomax algorithm. Of note, the Infomax algorithm is commonly used in the analysis of the fMRI data and looks for solutions to a mixed matrix in order to effectively separate multiple Gaussian source signals.

McKeown and colleagues first applied the ICA method as an fMRI analysis in 1998 (McKeown et al. 1998). In this study, the authors demonstrated that ICA could be applied to distinguish artifacts, non-task-related signal components, as well as continuous or temporary assignment-related fMRI activations, based on a weak assumption about their spatial distributions and without a priori knowledge about the time source.

**Fig. 2.1** Schematic diagram of the independent component analysis (Reprint with permission from Dai et al. 2013)



The temporal ICA (TICA) algorithm is commonly used under conditions where the times at which signals are collected are mutually independent from one another. In the TICA, data collected from the same voxel in  $L$  time points are regarded as a mixed component, so that the whole brain data is composed of  $M$  (the number of voxels) mixed components. TICA applied to whole brain data generates a series of independent time series and corresponding brain images.

Spatial ICA (SICA) is commonly used under the assumption that all components are mutually independent from one another, with each source represented as a spatially fixed pattern of activation. In the SICA, voxel-wise data throughout the brain collected at the same time point are regarded as a mixed component, so the whole brain data is composed of  $L$  (the number of time points) mixed components. SICA in whole brain data generates a series of independent images and corresponding time series.

### 2.2.3 Functional Connectivity Analysis

The concept of functional brain connectivity was proposed in early electrophysiological studies. In the early 1990s, Friston et al. introduced the concepts of functional and effective connectivity and applied them to issues in neuroscience (Friston et al. 1993a, b). Functional connectivity was initially defined as a temporal correlation between spatially remote neurophysiological events occurring in a neuroimaging time series. This definition was operational and provided a simple characterization of functional interactions. In 2000, Sporns et al. published a more precise definition of functional connectivity, stating that functional connectivity captures patterns of deviations from statistical independence between distributed and often spatially remote neuronal units, measuring their correlation/covariance, spectral coherence, and phase locking. Of note, functional connectivity does not provide any direct insight into how correlations are mediated (Sporns et al. 2000).

By contrast, effective connectivity can be defined as the influence of one neural system on another, occurring at either a synaptic or cortical level. Some studies have shown that structural equation modeling can be conceived as a linear regression model for effective connectivity, while dynamic causal modeling can improve analyses of brain connectivity to be more akin to analyses of regionally specific effects (Friston 1994; McIntosh and Gonzalez-Lima 1994; Buchel and Friston 1997; Mechelli et al. 2003).

There are two popular methods for functional connectivity analyses: the seed-based correlation analysis method and the multivariate analysis method, which includes ICA and principal component analysis (PCA) approaches. The specific processing steps for functional connectivity analysis include (1) image preprocessing, including realignment, spatial normalization, spatial smoothing, band-pass filtering, and covariate regression, (2) region-of-interest (ROI) selection to investigate specific regional correlations, (3) calculation of the correlation coefficients between the reference time course (in previous studies, the averaged time courses of voxels within a given ROI) and the BOLD time course from all of other brain voxels, and

(4) normalization of the distribution by applying Fisher's Z transform to the correlation coefficients.

In step 3 of this approach, correlation coefficients less than the given threshold are set to zero. The calculation is described as follows:

$$cc = \frac{\sum_{i=1}^N (r(i) - \bar{R}) \cdot (S_i - \bar{S})}{\sqrt{\sum_{i=1}^N (r(i) - \bar{R})^2 \cdot \sum_{i=1}^N (S_i - \bar{S})^2}} \quad (2.3)$$

where  $r$  is the reference time course,  $S$  is the signal for a given voxel,  $\bar{R}$  is the reference time course for a given voxel, and  $\bar{S}$  is the time series for a given voxel. The summation is performed for all time points. Because fMRI time series data can inform both temporal and spatial correlations, it can be expected that the distribution of correlation coefficients will be skewed due to intrinsic temporal and spatial correlations from the imaging method (Friston et al. 1994a; Lowe et al. 1998). The distribution of correlations can differ depending on the ROI selected as the reference for the correlation due to artifacts arising from cardiac, respiratory, or other physiological “noise” during volume collection (Lowe et al. 1998; Hampson et al. 2006).

In step 4, Fisher's Z transform is applied as follows:

$$F = \frac{1}{2} \ln \frac{1+r}{1-r} \quad (2.4)$$

At present, major neuroimaging studies of acupuncture primarily report acupuncture-induced activation patterns. Functional connectivity analyses can be applied to correlations analyses of multi-brain region activation following acupuncture stimulation in order to better inform the neural networks that underlie acupuncture effects.

#### 2.2.4 Time Series State Analysis Algorithm Based on the Change-Point Theory

As mentioned above, although the GLM approach has arguably become the most popular way to analyze fMRI data, it becomes impractical when the precise timing and duration of psychological events cannot be specified a priori. The hierarchical exponentially weighted moving average (HEWMA) model is an approach that allows the predicted signal to depend nonlinearly on the input, using ideas from statistical control theory and change-point theory to model slowly varying processes for which the onset times and durations of underlying psychological activity are uncertain. The HEWMA model is a multi-subject extension of existing EWMA models for individual participants (and accordingly a single time series), adapted to be applicable to a cohort analysis using a hierarchical model. The HEWMA method can thus be used for fMRI data analysis in a voxel-wise manner throughout the

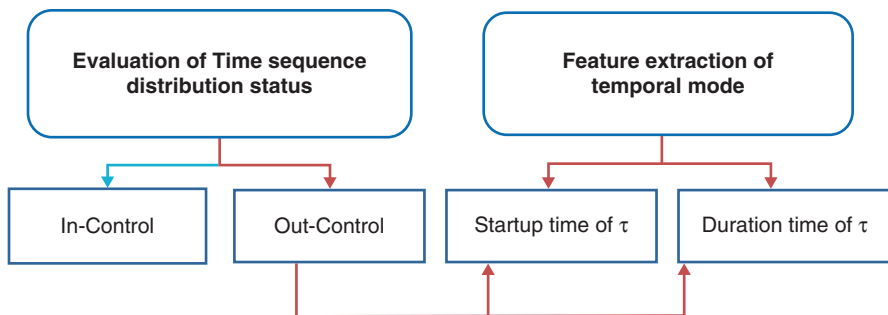


**Fig. 2.2** Schematic diagram of the time series state analysis algorithm based on the change-point theory (Reprint with permission from Dai et al. 2013)

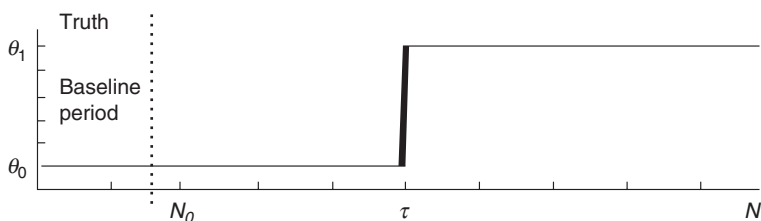


**Fig. 2.3** Schematic of the model of true activation (Reprint with permission from Lindquist et al. 2007)

brain, for ROI data, or for temporal components extracted using an ICA or a similar method (Wager et al. 2005; Lindquist et al. 2007).

A schematic diagram of the time series state analysis algorithm based on the change-point theory is shown in Fig. 2.2. Given a process that produces a sequence of observations  $\vec{x} = (x_1, x_2, \dots, x_N)^T$  (e.g., a fMRI time series), a two-state model can be produced where data is modeled as the combination of two normal distributions, one with mean  $\theta_0$  and covariance matrix  $\Sigma$  and the other with mean  $\theta_1$  and the same covariance. In the baseline acquisition period, the process generates a distribution of data with mean  $\theta_0$ , and the process in this state is considered to be in control. Observations maintain this distribution until the change point  $\tau$ , when the process changes (i.e., a new psychological state results in increased or decreased neural activity), generating fMRI observations from the second distribution with mean  $\theta_1$  (Fig. 2.3). In this second period, the process is deemed to be out-of-control or in the out-of-control state (Lindquist et al. 2007).

### 2.3 Acupuncture Neuroimaging Studies in Humans

Noninvasive brain imaging techniques, including positron emission tomography (PET) and fMRI, have provided the opportunity to examine the effects of acupuncture on brain activation. Accordingly, significant modulatory effects of acupuncture

have been identified at various levels throughout the CNS. This include the endogenous antinociceptive limbic networks (the cingulate cortex, insula, and hypothalamus) as well as higher-order cognitive and affective control centers within the prefrontal cortex and medial temporal lobe (the amygdala and hippocampus) (Wu et al. 1999, 2002; Hui et al. 2000, 2005; Kong et al. 2002; Zhang et al. 2003; Liu et al. 2004; Yoo et al. 2004; Pariente et al. 2005; Napadow et al. 2007). Here, we will review literature reporting the effects of acupuncture on brain activation.

In 1998, Cho et al. first reported that the vision-related acupoint stimulation at VA1, VA3, and VA8 could activate the primary visual cortex (Cho et al. 1998). However, acupoint specificity has not been fully supported by other fMRI studies. For example, while Cho's results were successfully reproduced by Siedentopf et al. (2002) using laser acupuncture, Gareus et al. (2002) failed to replicate these findings.

Neuroimaging data strongly suggest that acupuncture modulates many distributed cortical and subcortical areas of the brain involved in endogenous antinociception and the pain neuromatrix (Davis et al. 1997; Fields and Basbaum 1999; Hofbauer et al. 2001). Modulation of these areas may contribute to the therapeutic effects of acupuncture by shifting autonomic nervous system (ANS) balance and altering the affective and cognitive dimensions of pain processing (Peets and Pomeranz 1978; Clement et al. 1980). Wu et al. found that stimulation at ST36 produced specific increases in signal intensity of the hypothalamus and nucleus accumbens and specific decreases in signal intensity of the rostral anterior cingulate cortex (ACC), amygdala, and hippocampus (Wu et al. 1999). This evidence supported the hypothesis that acupuncture activates structures of the descending antinociceptive pathway and deactivates multiple limbic areas subserving the affective dimension of pain. Similarly, Hui et al. reported that needle stimulation at LI4 on either the right or left side produced consistent modulation of multiple cortical and subcortical limbic and paralimbic structures; moreover, this stimulation induced a wider range of negative signal changes in the limbic-cerebellar system such as the nucleus accumbens, amygdala, hippocampus, parahippocampus, hypothalamus, anterior cingulate gyrus (BA 24), temporal pole, ventral tegmental area, caudate, putamen, and insula (Fig. 2.4) (Hui et al. 2005). In addition, decreased neural responses were only identified in subjects that experienced deqi sensations not in the subjects who experienced pain sensations during needle manipulation. In contrast, two subjects who experienced sharp pain showed predominately increased signal intensity in the parahippocampus, ACC, posterior cingulate cortex (PCC), and putamen. Given that deqi is thought to play a pivotal role in the therapeutic effect of acupuncture (Takeda and Wessel 1994; Witt et al. 2005), observed decreases in activity in the limbic-cerebellar network may be a central characteristic of acupuncture's therapeutic effect.

Biella et al. (2001) demonstrated that true acupuncture at Zusanli (ST36) and Qi-ze (Lu 5) statistically increased regional cerebral blood flow (rCBF) in the ACC, bilateral insula, bilateral cerebellum, right superior frontal gyrus, and right medial frontal gyrus, whereas sham acupuncture (superficial needle insertion 1 cm lateral to each acupoint) increased rCBF in the raphe nuclei, hypothalamus, and left



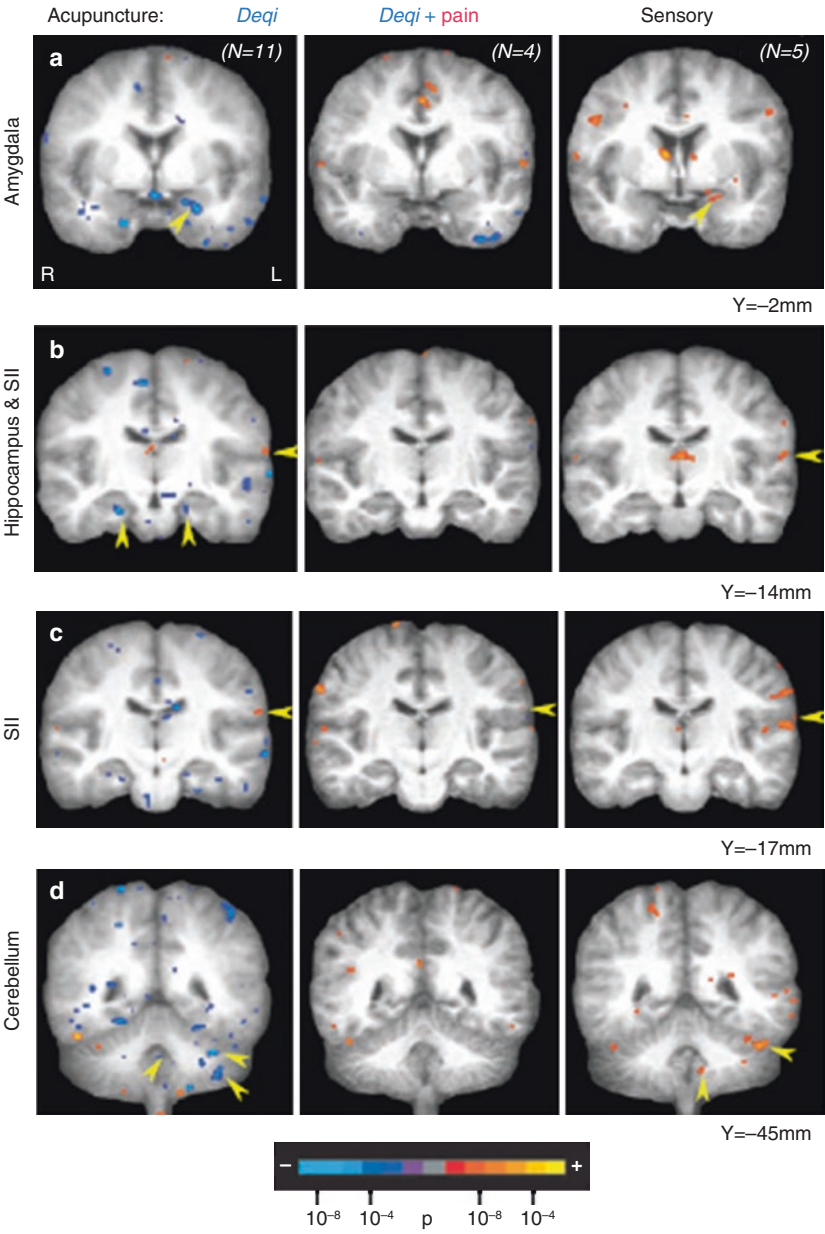


**Fig. 2.4** The influence of subjective sensations on fMRI signal changes on major limbic structures, the secondary somatosensory cortex (SII) and the cerebellum during acupuncture at ST36 (Reprint with permission from Hui et al. 2005). (Row **A**) The amygdala showed signal decrease with acupuncture *deqi*, increase with sensory stimulation, and no significant change with acupuncture mixed sensations. (Row **B**) The hippocampus, bottom arrows, showed signal decrease with acupuncture *deqi* and no significant change otherwise. (Row **C**) SII, also shown by the right arrows in Row **B**, shows signal increase under all three stimulations. Acupuncture, being a form of sensory stimulation, would be expected to result in signal increases in SII, which is in stark contrast to the widespread signal decreases during acupuncture *deqi*. (Row **D**) With acupuncture *deqi*, the cerebellum showed signal decreases in the vermis and lobules VI and VII





the somatosensory cortex (BA 3, 40) and PAG show distinct activity patterns in response to acupuncture (Liu et al. 2004). Yan et al. found that acupuncture at Liv3 (Taichong) and LI4 (Hegu) but not at sham acupoints activated areas in the middle temporal gyrus and cerebellum and deactivated areas in the middle frontal gyrus and inferior parietal lobule, with some degrees of acupoint specificity. That may reveal that acupuncture at acupoints induces specific patterns of brain activity and these patterns may relate to the therapeutic effects of acupuncture (Yan et al. 2005).

Some studies have demonstrated that different acupuncture manipulations result in different patterns of brain activation. Napadow et al. (2005) reported that EA (particularly at low frequency) produced more widespread fMRI signal increases than manual acupuncture and that all acupuncture stimulations produced more widespread responses than placebo tactile control stimulation. Furthermore, only EA generated significant activation in the anterior middle cingulate cortex (MCC) and pontine raphe area.

### **2.3.1 Sustained Effects of Acupuncture and Its Influence on fMRI**

To date, most neuroimaging studies of acupuncture have mainly focused on the acute impacts of acupuncture on brain activity, adopting the general linear model (GLM) for data analysis. Moreover, a large proportion of previous fMRI studies have employed a block experimental design, which is based on a stimulation-response model in which BOLD signal is assumed to change in response to stimulation and immediately return to the pre-stimulus state after the cessation of stimulation. With this approach, a specific stimulus sequence (i.e., design matrix) is used to define an ideal hemodynamic response function (HRF), which is convolved with the actual hemodynamic response and produces predictors of the BOLD response (Worsley and Friston 1995). Block design fMRI paradigms are useful for detecting activation in response to typical visual or motor tasks, as temporal changes in the BOLD signal conform to the stimulation-response model in these settings. However, a block design may be not valid in cases when a stimulus-response behavior has not been confirmed, as in the case of acupuncture stimulation.

Acupuncture has been shown to exert sustained effects on brain activity even after the cessation of needle stimulation (Price et al. 1984), suggesting that acupuncture effects may have time-variant properties that are acupoint specific. To this end, many clinical reports have indicated that acupuncture produces therapeutic effects that long outlast the duration of actual therapy (Beijing and Nanjing Colleges of Traditional Chinese Medicine 1980). A psychophysical analysis by Price et al. (1984) also suggested that the analgesic effects of acupuncture peak long after the completion of a needling session. On the hypothesis that acupuncture has sustained effects, the temporal aspects of BOLD responses to acupuncture are likely to violate the assumptions of block design GLM estimates (Fig. 2.6) (Bai et al. 2009b) in that

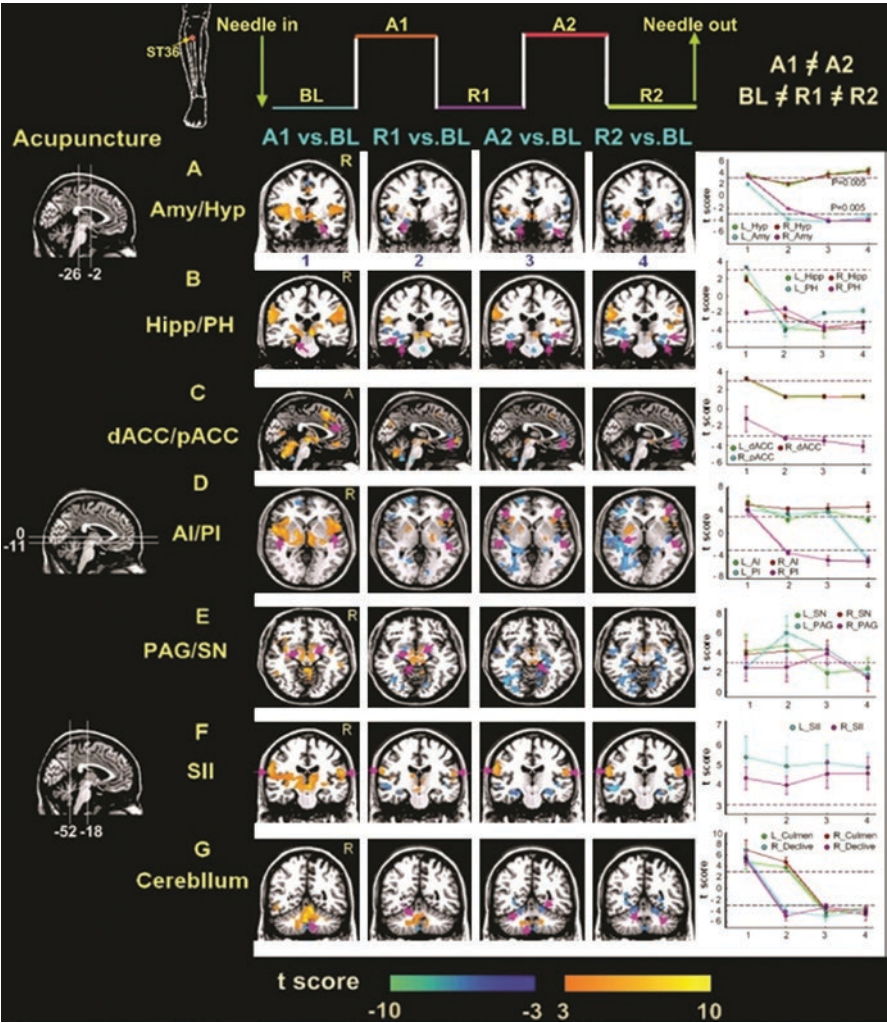
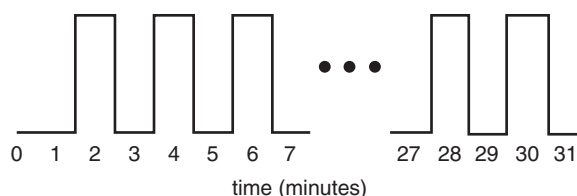


**Fig. 2.6** Activity patterns of representative areas in different epochs of multi-block following acupuncture stimulation at ST36 (Reprint with permission from Bai et al. 2009b). Corresponding *t*-values of representative regions in different periods are also indicated. Error bars indicate the standard error of the mean. (A, B) The amygdala (Amy), hippocampus (Hipp), and parahippocampus (PH) exhibited weakly positive responses in the first stimulation (A1) that decreased to below baseline level thereafter. (C) Early positive and negative signal responses were notable in the dorsal and pregenual anterior cingulate cortex (dACC and pACC), respectively, in sequential conditions. (D, F) The anterior and posterior insula (AI and PI) and secondary somatosensory cortex (SII) exhibited persistently increased responses during the whole trial. (A, E) Episodic responses were primarily distributed in the hypothalamus (Hyp) and brainstem structures (periaqueductal gray, PAG; substantia nigra, SN). The greatest positive activity emerged in R1 and plateaued in A2 but was nonsignificant. (G) Early responses in the cerebellum (culmen and declive) were positive and later became negative

**Fig. 2.7** An fMRI block design paradigm consisting of alternating 1-min stimulation (ST36 or sham acupoint) and rest blocks (Reprint with permission from Napadow et al. 2009b)



relevant BOLD responses are unlikely to return to baseline after initial stimulation. Indeed, an investigation using an ICA provided direct evidence that interleaved resting epochs in the block design paradigm retain acupuncture-related changes (Zhang et al. 2009). On the basis that the temporal profile of acupuncture is slow to develop and resolve, more appropriate design paradigms and statistical models should be selected in future studies in order to elucidate the actual effects of acupuncture.

One major obstacle to the multi-block design is the difficulty of distinguishing between brain activity related to acupuncture manipulation itself (e.g., sensation, attention, and cognition) and activity associated with its sustained effects. Napadow et al. (2009a) adopted a long duration (>30 min) stimulus paradigm and compared ST36 acupuncture with sham point acupuncture to evaluate time-variant brain responses (Fig. 2.7). They found that ST36 verum acupuncture modulated activity in the substantia nigra, nucleus raphe magnus, locus coeruleus, nucleus cuneiformis, periaqueductal gray, and limbic areas, whereas both stimulations produced linear decreases in the time-variant activation of sensorimotor brain regions (i.e., the SII, insula, and premotor cortex). These data indicated that acupuncture produces to both early (immediate) and late (30 min after the start of stimulation) phases of brain activation. To address this possibility, Qin et al. (2008) proposed a novel experimental paradigm, non-repeated event-related fMRI (NRER-fMRI), to explore the prolonged effects of acupuncture on resting-state brain networks. Compared with the acupuncture at a nearby non-acupoint, ST36 acupuncture produced higher-level correlations among amygdala-associated networks; these areas mainly included limbic/paralimbic areas (the ACC and insula) and brainstem structures (the PAG) (Fig. 2.8). Similarly, acupuncture but not sham stimulation produced increased connectivity in the default mode network and sensorimotor network (Dhond et al. 2007), including the medial temporal lobe, PAG, and supplementary motor area (SMA). Connectivity between the hippocampus and DMN was also correlated with parasympathetic output following acupuncture stimulation in the abovementioned study. These data indicated that autonomic modulation might represent an important therapeutic mechanism of acupuncture leading to sustained effects, which is consistent with what is known regarding autonomic efferent nerve activity and the analgesic effects of acupuncture (Haker et al. 2000; Hsu et al. 2007; Sakai et al. 2007). In further support of this hypothesis, Baliki et al. (2008) reported differences in resting-state brain functional connectivity between individuals with chronic pain and healthy control subjects and proposed that differences were related to the cognitive and affective components of chronic pain. Future exploration of the alternating interplay between external acupuncture intervention and the reorganization of



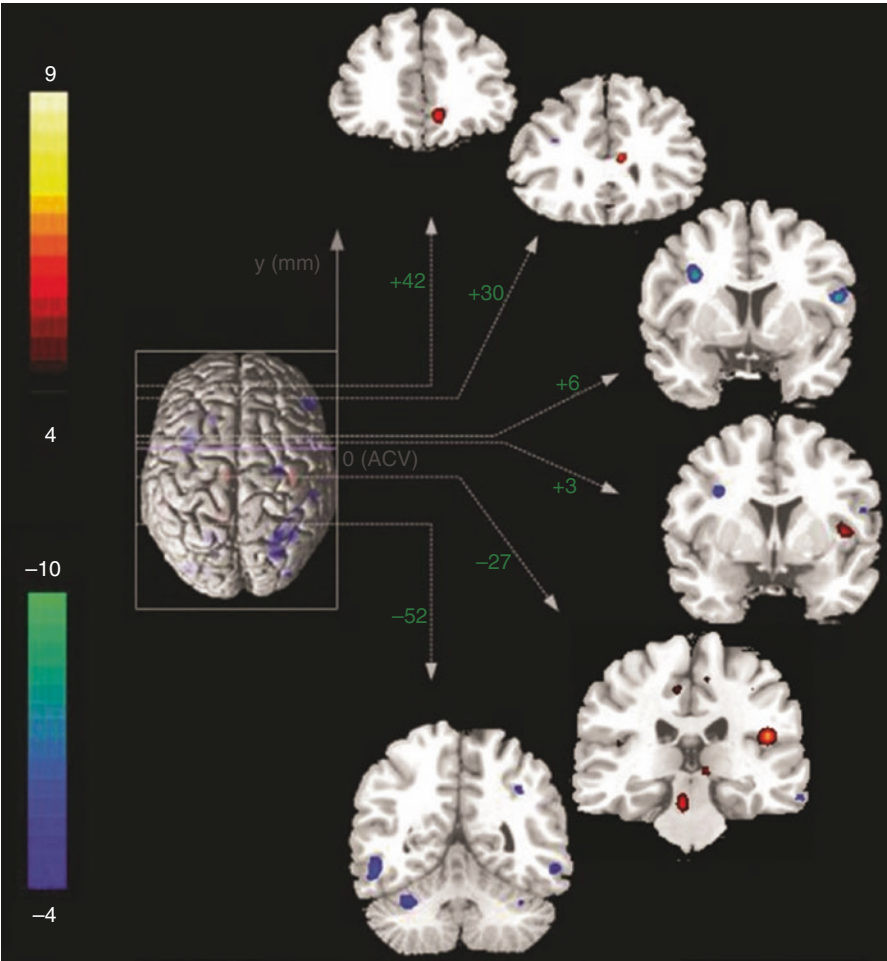


**Fig. 2.8** Acupuncture enhanced activity correlations between the amygdala and the insula, anterior cingulate cortex, and periaqueductal gray poststimulus (Reprint with permission from Bai et al. 2009a), whereas sham stimulation enhanced activity correlations between the amygdala and the secondary somatosensory cortex and cerebellum. ACV, anterior commissure verticalization

resting-state brain networks in chronic pain patients will better inform our understanding of the mechanism of acupuncture analgesia.

If acupuncture exhibits temporally delayed effects, an understanding of its temporal properties is crucial. One pioneer study developed a novel approach (defining separate models) to evaluate dynamic signal changes between baseline activity and post-acupuncture neural activity in sequential epochs within a multi-block design (Bai et al. 2009b). The results showed that ST36 acupuncture induced time-varied response patterns in limbic-cerebellar and brainstem structures (Fig. 2.6). Moreover, it was noted that some regions only responded to initial acupuncture stimulation (i.e.,

the PCC), while others exhibited increasing or tapering activities for the duration of the experimental session (i.e., the PAG and rostral ventromedial medulla [RVM]). Further, other brain areas showed sustained responses (i.e., the insula) and continuously exerted controlling and coordinating influences throughout the scan. Limbic and brainstem areas have been indicated to support endogenous antinociceptive mechanisms as part of the pain neuromatrix. In addition, evidence from animal studies suggests that acupuncture analgesia is supported by endogenous opioidergic and/or monoaminergic antinociceptive networks (Hoffman et al. 2005). The PAG and RVM together serve as one such mechanism that modulates ascending nociceptive responses by promoting the release of endogenous opioids (Napadow et al. 2005). The RVM has distinct functional populations of neurons that inhibit (off cells) and facilitate (on cells) nociceptive transmission (Haws et al. 1989; Tortorici and Vanegas 1994). Accordingly, the PAG-RVM network may function as a unit to exerting discrete global control over dorsal horn pain transmission in the context of acupuncture analgesia. In addition, PAG activity is facilitated by top-down processes originating in higher centers such as the insula and ACC (Fields et al. 1991; Urban and Gebhart 1999; Millan 2002; Porreca et al. 2002). These areas, along with limbic regions including the hippocampus and amygdala, comprise the descending antinociceptive pathway. Thus, it can be theorized that the mechanism of acupuncture analgesia may relate to altered pain perception mediated by inhibiting the antinociceptive action in the affective pathway while mobilizing the descending mechanisms by controlling the transmission of nociceptive signals to the brain.

---

## 2.4 Brain Network Analysis Methods

### 2.4.1 Graph Theory in Brain Network Analysis

Brain systems are frequently comprised of smaller, dynamic, and highly interacting subsystems. Graph theory is one method used to study the general features of these systems. In the context of graph theory, dynamic subsystems are represented as network nodes, and subsystem interactions are represented as network edges. Graph theory model differs from traditional network analysis methods in that it is more focused on subsystem interactions than subsystem structure and function.

#### 2.4.1.1 Common Network Parameters According to Graph Theory

The principle of graph theory is summarized in Fig. 2.9. A network consists of two sets: set  $V$  of nodes and set  $E$  of edges.  $N$ , the size of set  $V$ , represents the size of the network. Homogeneity among the elements of set  $V$  reflects whether nodes in a given network have the same properties. Element  $\text{link}_{ij}$  in set  $E$  is a combination of two elements, node  $i$  and node  $j$  in set  $V$ , and indicates that there is an edge between node  $i$  and node  $j$ . If  $(k, j)$  is an ordered pair, the network can be seen as directed; otherwise, it is undirected. If each element in set  $E$  has a different value, the network is a weighted network; otherwise, it is unweighted. Generally, an edge that connects with itself without passing other nodes does not exist in set  $E$ , which means that the

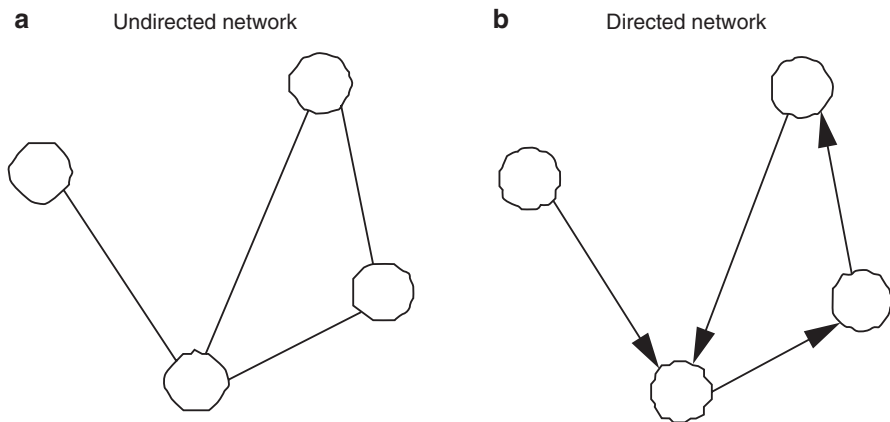


**Fig. 2.9** Different kinds of networks according to graph theory (Reprint with permission from Dai et al. 2013). (a) Undirected network; (b) directed network

combination of  $(j, j)$  does not exist. Moreover, in an undirected network, there is only one connected edge between two different nodes.

In a network, the path between two nodes is defined as a non-repetitive sequence of nodes and edges passed from one node to another. The length of the path is defined as the sum of the length of mid-edges in the sequence. The shortest length of path is called as characteristic path ( $L$ ). If any two nodes can be reached by a path, the network is a connected network; if a network cannot be connected as a whole, the largest connected network in it is studied and used to make generalizations.

The degree value  $k_i$  of any node of a network indicates the sum of nodes that are directly connected with the given node. The degree value can therefore be obtained by summing over the elements of line  $i$  in an adjacency matrix; that is to say,  $k_i = \sum_j \in va_j$ . If the network is a directed network, the degree of nodes can be divided into two parts, in-degree  $k_i^{\text{in}} = \sum a_{ij}$  and out-degree  $k_i^{\text{out}} = \sum a_{ij}$ , such that the total value of the degree is  $k_i = k_i^{\text{in}} + k_i^{\text{out}}$ . The degree value accordingly represents the role that a given node plays in a network.

One of the most fundamental properties of a network is degree distribution, which is the probability of randomly selecting a node whose degree value is  $k$ . In empirical analysis, the degree distribution is generally represented by the ratio of the number of nodes representing the degree value  $k$  to the total number of nodes in a network. Research has shown that the degree distribution of a random network produced by the ER model of Erdos and Renyi follows a Poisson distribution. However, in many complex networks abstracted from real systems (e.g., scientific collaboration networks), degree distributions all follow power law distributions.

Characteristic path length is an important parameter used to describe the inside structure of networks and provides the optimal path for information transfer from one network node to another. This parameter plays a significant role in information transmission and network communication (Pastor-Satorras and Vespignani 2004;



Reijneveld et al. 2007). Moreover, characteristic path length can reflect the efficiency of information transmission of the network on a global scale. The characteristic path length matrix can be used to describe the characteristic path length  $l_{ij}$  of any two nodes in a given network, defining the diameter of the network as the longest characteristic path length contained therein. Network mean characteristic path length  $L$  describes the average value of the characteristic path length for any two nodes in a given network; that is,  $L = 1/N(N-1) \sum_{i,j \in V, i \neq j} l_{ij}$ . In general, the characteristic path length matrix is calculated in a connected module. This is because, if a network does not contain unconnected nodes, the characteristic path length of two nodes is infinite. To this end, Newman (2003) developed a method for measuring the mean characteristic path length using the reciprocal of the harmonic average.

The clustering coefficient is another significant parameter to measure the characteristics of a network and is applied to measure the possibility that two nodes adjacent to a third node are also neighbors (Watts 1999). The value of the clustering coefficient  $C_i$  of node  $i$  equals the ratio of the number of edges ( $e_i$ ) existing between adjacent nodes to the total possible number of edges among them  $k_i(k_i-1)/2$ , which

is  $C_i = \frac{2e_i}{k_i(k_i-1)} = \frac{\sum_{j,m} a_{ij}a_{jm}a_{mi}}{k_i(k_i-1)}$ . The average of the clustering coefficient of all

nodes in a given network is the clustering coefficient of the network; that is,

$$C = \langle C_i \rangle = \frac{1}{N} \sum_i C_i.$$

A final important network parameter is global efficiency  $E_{\text{glob}}$ , which can be described as  $E_{\text{glob}} = 1/N(N-1) \sum_{i,j \in V, i \neq j} 1/l_{ij}$ , in which  $N$  represents the number of nodes in the network and  $l_{ij}$  is the characteristic path length of two nodes in the network. The cost of the network is defined as  $k_{\text{cost}} = 1/N(N-1) \sum_i k_i$ , in which  $N$  represents the number of nodes in the network and  $k_i$  represents the degree value of node  $i$ .

#### 2.4.1.2 The Topological Properties of Small-World Networks and Scale-Free Networks

Complex networks typically fall into two categories: small-world networks (Watts and Strogatz 1998) and scale-free networks (Barabasi and Albert 1999). In the real world, most complex networks have both small-world and scale-free properties at the same time.

The small-world network model was first put forth by Watts and Strogatz (1998). The small-world network has a combination of regular and random network properties and was welcomed with much enthusiasm by the scientific community. In a regular network, the characteristic path length between any two nodes will increase if the network size increases, but the clustering coefficient will not decrease at the same time. In contrast, in a completely random network, the characteristic path length between nodes is short, and the network clustering coefficient is also small. Studies on real-world dynamic processing have shown that there are many shortcuts and edges connecting different areas in a given network, which makes it easier and

faster to transfer information between two nodes that are far apart. Although the size of a network might be large, the characteristic path length between nodes can be relatively short, such that the mean characteristic path length  $L$  of the network can be described as a geometric logarithm that increases with the growth of the network size  $N$ ; that is,  $L \propto \log(N)$ . Of note, the clustering coefficient of a regular network is larger than that of a random network.

Social psychologist Stanley Milgram proposed the concept of six degrees of separation in 1967 based on experimental data statistics (Milgram 1967; Travers and Milgram 1969; Korte and Milgram 1970; Dodds et al. 2003). The six degrees of separation theory states that, in a social network, two strangers can build a connection based on a limited number of acquaintances. That is, more than six steps of separation are required to meet a complete stranger. This phenomenon is also called the small-world phenomenon and exists in many networks (Latora and Marchiori 2001, 2003). Watts and Strogatz pioneered the description of small-world network characteristics, pointing out that a small-world network has a small mean characteristic path length and, unlike the corresponding random network, a large clustering coefficient. These characteristics can be expressed as follows:  $\gamma = C_{\text{net}}/C_{\text{rand}} \gg 1$ ,  $\lambda = L_{\text{net}}/L_{\text{rand}} \sim 1$ , where rand represents a random network and net represents a real network. From this definition, it can be seen that networks with small-world characteristics have efficient partial and global information processing mechanisms (Stanley 1971).

The concept of the scale-free network was initially proposed by Barabasi and Albert (1999). Barabasi and Albert found that the degree values of many networks in the real world follow a power law distribution; examples include Internet networks, scientific collaboration networks, metabolic networks, and telephone networks. In these networks, the average degree cannot act as a characteristic scale of the network. Therefore, these networks are referred to as scale-free. Moreover, the ability of the node degree to follow a power law distribution is a scale-free characteristic. However, of note, many networks in the real world can follow other distributions including the exponential distribution, Gaussian distribution, and combination distributions.

The power function is a curve that slows gradually, permitting the existence of nodes which have larger degrees in the network. These nodes are hub nodes and can significantly influence the characteristics and functions of the network.

#### 2.4.2 The Application of Graph Theory in Neuroscience Studies

The brain is the most perfect dynamic information processing system known to man. A body of previous research has led to the conclusion that the cerebral cortex is comprised of multiple neural clusters that have partial functional specificities. Neural clusters interact dynamically with one other and build different circuits to support a variety of cognitive activities. An important feature of brain network function is the ability to achieve a balance between functional differentiation and integration. While several experiments in neuroanatomy and electrophysiology have produced information about the data of the channel cortex (Hellwig 2000; Kotter

2001), relatively little is known about the global organization and function of complex functional networks in the brain. New computational methods have been innovated for the study of brain connectivity; of these, graph theory analysis is one useful tool for studying brain network organization principles and characteristics from a global angle.

Indeed, the use of graph theory has begun to flourish in the field of neuroscience, but additional high-quality implementations are required. Previous studies have focused on brain activities during cognitive tasks and considered different regions as different nodes in a complex interactive network. In these studies, interrelations and functional correlations among different brain regions serve as network edges.

Watts and Strogatz (1998) used the graph theory method to identify small-world characteristics in the nervous system. A complex network quantitative method was employed in *C. elegans*, where each neuron was regarded as a node and synaptic connections were regarded as edges. This resulted in a directed network consisting of 282 nodes and 2462 edges. Using this model, Watts and Strogatz discovered that the topological structure of the *C. elegans* network was neither random nor regular network but instead had small-world features.

Salvador et al. (2005) was the first to employ graph theory for the analysis of brain fMRI data. The whole human brain was divided into 90 ROIs (45 for each cerebral hemisphere), and correlations between the resting-state BOLD signals of any two regions were calculated to build the functional network. Salvador and colleagues subsequently analyzed the clustering coefficient and mean characteristic path length of the resultant network and confirmed the presence of small-world characteristics in the resting-state human brain. The authors also identified the presence of subnetworks with long-distance functional connectivity using a cluster analysis.

Achard and colleagues studied the properties of brain networks at different frequencies using wavelet transformations (Achard et al. 2006) and found that small-world characteristics were most notable at low frequencies (0.03–0.06 Hz). Moreover, the degree distributions of human brain networks were found to follow a truncated power law distribution. Fair et al. applied graph theory to developmental neuroscience research and found that human brain development reveals the process of network organization (Fair et al. 2007). It was found that the merging and separation of brain network modules occurred simultaneously, decreasing the number of short edges and increasing the number of long edges over the course of development (Fair et al. 2009). The synthesis of the default network was directly observed during development (Fair et al. 2008).

The above studies all regarded information from one brain region as a single network node. Instead, van den Heuvel et al. studied the brain network at a voxel level (van den Heuvel et al. 2008) and found that voxel-level brain networks also exhibit small-world characteristics. Accordingly, it can be interpreted that the characteristics of human brain networks are robust. However, the power law distribution of degree values in voxel-level brain networks was found to diverge from that in brain region-level networks.

In recent years, graph theory has also been applied to study brain network abnormalities in patients. Supekar et al. (2008) discovered that small-world characteristics were diminished in Alzheimer's disease patient brain networks, specifically manifesting as smaller clustering coefficients with respect to healthy brain networks. This variation was proposed as an index for distinguishing patients from healthy individuals. However, in work performed around the same time, He et al. (2008) demonstrated larger clustering coefficients and mean characteristic path lengths in patients relative to healthy individuals.

Liu et al. (2008) used graph theory to study network characteristics in schizophrenic patients and found that both clustering coefficients and network efficiency were decreased, while the characteristic path length was increased in patients relative to healthy control subjects. In attention-deficit/hyperactivity disorder research by Wang et al. (2009), partial increases in network efficiency were noted although global efficiency was unchanged. Most recently, in 2009, Liu and colleagues evaluated brain network characteristics in individuals with heroin addiction (Liu et al. 2009). The results showed that individuals with heroin addiction retained small-world brain network characteristics but the small-world parameter  $\gamma$  was markedly decreased with respect to healthy control subjects.

### 2.4.3 The Application of Graph Theory in Acupuncture Studies

In recent years, researchers have begun to apply graph theory to the study of acupuncture (Liu et al. 2010; Qin et al. 2011). The results of these studies showed that after acupuncture therapy, brain network connectivity exhibited time-variant alterations, indicating a lasting effect of acupuncture on network reorganization. Differences noted between the brain network connection modes of the acupuncture and control groups indicated that the anterior insula was significantly involved in acupuncture's effect. In future research on the mechanisms of acupuncture, graph theory should be employed to provide further insight into the effects of acupuncture on signal processing efficiency, brain network connectivity, and network structure.

### 2.4.4 Analytical Algorithms Based on Pattern Classification

A fundamental content of cognitive neuroscience is to determine how information is represented in neural activation patterns. For this purpose, fMRI is an invaluable tool. Tens of thousands of millions of voxels of data can be produced by fMRI within a matter of seconds; however, the large sizes of these datasets and high levels of inherent noise complicate the use of these datasets for informing cognitive processes (Norman et al. 2006). Acupuncture stimulation usually produces the synchronous activation multiple voxels, resulting in temporal patterns on time series. As mentioned earlier in this chapter, the GLM method is a common analysis approach, but this method is not useful for multi-voxel analyses. Therefore, alternative data analysis

methods are required to process this type of fMRI data, particularly for the purposes of acupuncture research.

As mentioned in Chap. 1, Hui and colleagues offered the notable hypothesis that acupuncture produces limbic system deactivation and published several high-level academic papers on the subject (Hui et al. 2000; Smith et al. 2005). This hypothesis theorizes that acupuncture can cause widespread signal deactivation, especially in the limbic system-cerebellar neurocyte, as part of a complex multisystem effect. To address this hypothesis, it is necessary to focus on characteristics of the spatial distribution of brain activation mode under the condition of acupuncture stimulation. Multi-voxel pattern analysis (MVPA) provides a solution to achieve this purpose. MVPA is a data-driven analysis method that does not restrict the analysis of fMRI data to the voxel level. Specifically, MVPA attempts to improve the extraction of neural response activation areas by integrating information on a multi-voxel level. Compared with traditional methods for fMRI analysis, MVPA offers several benefits: first, MVPA provides increased sensitivity; second, increased sensitivity afforded by MVPA methods makes it feasible to measure the presence/absence of cognitive states based on only a few seconds' worth of brain activity data. If the cognitive states in question are sufficiently distinct from one another, discrimination can be made with acceptable statistical significance. MVPA methods can also be used to characterize how these cognitive states are represented in the brain (Norman et al. 2006). Machine learning theory supplements MVPA with a variety of classification algorithms, such as neural network, linear discriminant analysis, and support vector machine algorithms. A brief introduction of basic steps involved in the MVPA method is provided in Fig. 2.10 and summarized here.

1. A multi-block experimental design is used for feature selection (Fig. 2.10a). During scanning, the subject receives two types of visual stimulation: in the example, one is a picture of a bottle, while the other is a picture of a shoe. The purpose of this design is to investigate whether it is possible to judge the kind of stimulation that the subject is receiving according to the gray value of voxels in the cerebral cortex on fMRI data. Therefore, to extract special pattern, we need to select a group of voxels. The gray value of a group of voxels is used to build the feature vector of the present brain activation mode. Moreover, the constructed feature vectors are used in the next step of pattern classification in order to allow the classification of brain activation states.
2. Next is integration of the collected fMRI data (Fig. 2.10b); that is, the fMRI time series of the whole brain for every subject is divided and recombined according to stimulation condition. This is the matrix of feature vectors. Inside of feature vectors are the signal values of voxels in the selected voxel group at specific time points. Given that the stimulation conditions correspond with every feature vectors, the characteristic data must next be divided into two sets: a training set and testing set.
3. Next, the training set is used for to train the sorting machine (Fig. 2.10c). Obtaining discriminant forms of classification and entering the new feature vectors, we can estimate the category of each feature vector.

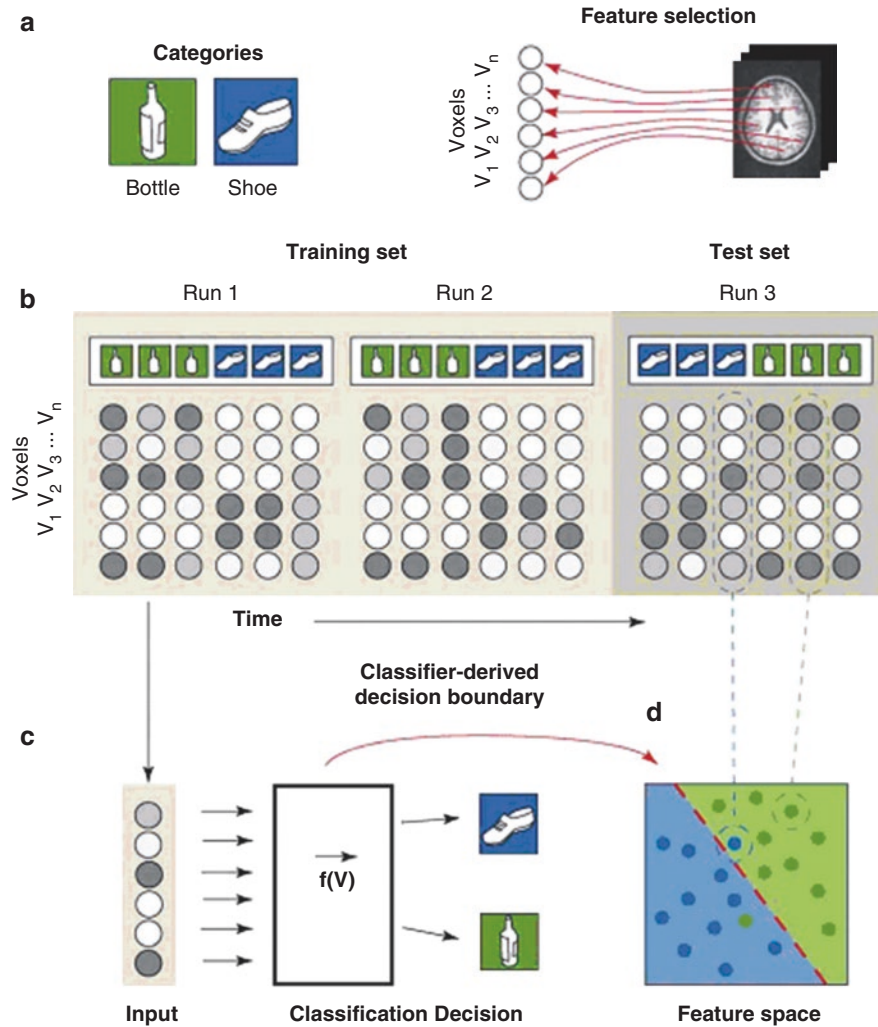


**Fig. 2.10** A summary of the multi-voxel pattern analysis method (Reprint with permission from Dai et al. 2013)

4. Next, the trained sorting machine defines a high-dimension voxel model space (compressed into two-dimensional space for the purpose of display; Fig. 2.10d). The red imaginary line is the boundary for classification. Every point in Fig. 2.10d corresponds to a feature vector; that is, a brain activation mode at a specific time point (green and blue correspond to the two stimulation conditions, respectively). The color of the background represents the class of the field to which the feature vector selected by the sorting machine belongs. In the picture, this includes an activation mode that is correctly classified as the bottle picture stimulation (indicated by the green dotted line) and an activation mode classified as the shoe picture stimulation.



Of note, in order to avoid signal deficiencies when applying the MVPA algorithm, smoothing of the voxel signal space should generally be omitted from the fMRI preprocessing protocol; although averaging spaces is an efficient way to decrease noise, it can also obscure meaningful activation signals that can be used to distinguish activation modes, including signal related to the judgment of information and subtle texture patterns of the space mode.

Selection of the sorting machine is another important consideration when applying the MVPA algorithm. As abovementioned, machine learning theory provides a wide variety of classification algorithms for MVPA. The MVPA method commonly adopts a linear discriminant machine (e.g., neural network, linear discriminant analysis, or support vector machine), which calculates the weighted average of voxel gray value, inputs the weighted average as a discriminant equation, and then confirms the category to which the pattern belongs using an effective threshold. Although traditional pattern analysis theory indicates that a nonlinear training machine has a wider range of application than linear training machines, there is no evidence to support this concept in the context of MVPA (Cox and Savoy 2003). Moreover, some research indicates that the results obtained from nonlinear machine methods are more difficult to interpret (Kamitani and Tong 2005). Therefore, a linear support vector machine is recommended for investigating the corresponding neural activation modes stimulated by acupuncture.

According to the MVPA method, characteristics are attributed to large groups of voxels such that even slight responses can lead to the observation of gradual changes under different conditions. Examples of experimental contexts where MVPA has been applied successfully include distinguishing between the visual observation of different object categories, invisible differences between line orientations, and natural scenes. MVPA can also be used to draw conclusions about the neural manifestations underlying a given phenomenon or behavior (Oosterhof et al. 2011). For this purpose, some researchers have combined a ROI-based analysis with the MVPA approach to study characteristics of activation among groups of specific voxels. Although an ROI-based method is appropriate in some cases, the a priori designation of ROI edges is a complex procedure when used in tandem with MVPA. When comparing voxel-based and surface-based methods, it is noteworthy that surface-based methods can provide higher-quality alignment and easier visualization.

The searchlight method is another way in which MVPA can be used to sensitively identify regions encoding specific stimulation types. By moving a searchlight among every voxel, a map of information about the different criteria of interest in the experiment is provided. Conventionally, the searchlight is conceived as a volume sphere that is small enough to have functional anatomical significance with respect to the surface of the cerebral cortex. For information mapping, Oosterhof et al. (2011) performed voxel by utilizing a cortical surface reconstruction. This method diverges from traditional volume-based MVPA in two manners: first, cortical surface reconstruction doesn't utilize voxels that are not a part of the gray matter identified by the anatomical scan. Second, it uses a surface-based geodesic distance metric to define neighborhoods of voxels and does not select voxels across a sulcus.



Additional researches are required to understand how these two differences influence the validity of category creation and the spatial characteristics of the obtained information map. Oosterhof et al. (2011) applied this method to fMRI data obtained while subject pressed a button with one of their fingers. Surface-based MVPA, especially the information mapping component, was more sensitive than a volume-based approach for measuring information content in this experiment. In addition, surface-based MVPA provided more accurate spatial selectivity.

Currently, the use of fMRI to study acupuncture mainly employs a multi-block experimental design. Similar to the former (Hui et al. 2000; Cox and Savoy 2003; Kong et al. 2009), we can apply multi-block experimental design but applied MVPA at each stimulation or rest condition.

Pattern selection is one of the most important steps for the MVPA method, as the final result largely depends on this process. Therefore, it is necessary to extract the feature vector which best reflects the spatial distribution of the central nervous system activation mode; that is, the gray voxel value vector most likely to be included in activated regions. There are two main methods of selecting the feature vector for this purpose:

1. Find out which clusters of the cerebral cortex will be activated under some specific condition based on a priori information (e.g., neuroanatomy or physiology) to determine the ROI. For example, if the experiment only involves visual stimulation, researchers may select a region from occipital lobe to make the feature vector.
2. Base the selection on the statistical result of a traditional general linear model. Application of a traditional general linear model data analysis can yield a statistical parametric map. In this map, every voxel has a corresponding value of  $t$ , where  $t$  is used to reflect the degree of activation of voxels. Therefore, the  $t$ -value can be utilized to make an appropriate threshold; voxels with a  $t$ -value higher than the threshold can be put into the voxel group used for extracting the feature vector. For traditional fMRI analysis methods, the statistics of any voxel groups can be used as a basis for selecting the feature vector.

Of note, pattern selection according to a traditional general linear model still has many problems. Although the threshold is quite low during the process of feature vector extraction, if we consider voxels which were not selected as a whole, these regions may contain information relevant to the stimulation-specific activation mode. Therefore, we can use multi-voxel pattern selection method to take the place of the single-mask pattern selection method. Importantly, multi-voxel pattern selection can consider information from whole groups of voxels. Of course, because of the large number of voxels that comprise the entire cerebral cortex, it is computationally difficult to consider all voxels in the brain, even with a multi-voxel pattern selection method. Given that interest is only in specific voxels that can distinguish a given central nervous system activation mode, and considering the functional connections between adjacent voxels, searchlight is an appropriate choice as a pattern selection method (Mitchell et al. 2004).

Comparing the analysis results of MVPA and those obtained from a traditional general linear model, it is clear that MVPA provides a more meaningful basis for determining acupoint specificity. Although the traditional general linear model method has some utility, it lacks sufficient sensitivity and the ability to detect subtle differences in spatial activation patterns. MVPA is a preferable and sufficiently powered method for identifying differences in spatial activation between true and sham conditions in acupuncture studies.

---

## 2.5 The Temporospatial Encoding of Acupuncture Effects on Brain Networks

The topological structure of a brain network has a significant effect on its function and dynamic behavior. In neural networks, topological structure refers to the paths for movement of neural information. Anatomical research has verified some fundamental properties of cortical connections; local connections between nerve cells are on the order of a few 100 mm (Le et al. 1991). In addition, long-distance neural connections exist inside the brain, connecting different regions in the cerebral cortex. These long-distance neural connections allow rapid interactions among distant brain regions (Kong et al. 2002). Indeed, these local and long-distance connections provide a good balance between specificity of local brain function and global brain functional integration. However, the experimental quantization and measurement of global properties are still in its early stages of development, and new computing methods for assessing large amounts of information about brain functional connections are a great need. This need is emphasized by a shifting focus of research to functional brain network connectivity (Albert et al. 2000; Achard et al. 2006; Achard and Bullmore 2007; Dhond et al. 2008; Buckner et al. 2009; Bullmore and Sporns 2009; Wang et al. 2010).

Given the complex effects of acupuncture on multiple systems in the human body (Rainville et al. 1997), it is logical that a similar complexity is encountered in the study of acupuncture effects on the brain. In recent years, the “point-to-point” simple research approach of examining simple correlations between spatial activation and acupuncture has proven to be insufficient. Recently, a top acupuncture research group at Massachusetts General Hospital published the first paper about acupoint specificity from a network perspective (Dhond et al. 2008). In this paper, obvious differences in functional brain networks were identified between acupoint and sham (non-acupoint) stimulation conditions. In the same year, a preliminary report was published on acupoint specificity and the a priori information network (Qin et al. 2008). In this article, a clear specific effect of Zusanli point acupuncture was demonstrated on amygdala brain networks. These results are perhaps the first to support the theory of acupoint specificity in a scientifically and methodologically robust manner.

In this section, we have considered the effects of acupuncture on the central nervous system as temporally complex with network-level impact and recommended the application of graph theory to describe complex correlations and system-level

changes in the brain. By mapping the activities and functional connections of brain regions involved in acupuncture and compiling these interactions into a complete network, we can gain a better understanding of acupuncture and the ways in which it can be used in the clinical context. Further, graph theory analyses offer a unique possibility for novel perspectives on medical diagnosis and treatment. Improved understanding of topological network structure and subsystem organization in the brain will provide a new path for acupuncture research.

---

## 2.6 Summary

Acupoint specificity lies at the core of traditional acupuncture theory; the clinical effectiveness of acupuncture is said to depend upon the specific placement of the needles at designated acupuncture points (Kaptchuk 2002). However, neuroimaging evidence supporting the specificity of acupuncture modulatory effects is conflicting. Previous studies have only investigated the spatial distribution of neural responses to acupuncture at specific acupoints, such that temporal information and more complex network-level information have been ignored. As aforementioned, the kinetics of acupuncture is inherently complex and time dependent. An accurate interpretation of acupuncture actions may therefore depend on how effectively we can characterize the nature of temporal variations in brain responses. Moreover, a majority of previous acupuncture neuroimaging research is fraught with methodological challenges, such that these studies may not have sufficiently addressed the complexities of the therapeutic mechanisms of acupuncture. Variability in needling technique, deqi sensations, design paradigm, differences in neuroimaging hardware and software, and data post-processing methods (Smith et al. 2005; Kong et al. 2007) are all likely to account for reported differences in brain responses between studies. Therefore, it is critical to define a standardized system for reporting the details of acupuncture manipulation (MacPherson et al. 2002). In addition, it is necessary to improve and standardize the use of sham or control stimulations in acupuncture studies. A particularly useful approach is the retractable non-penetrating sham needle (Streitberger and Kleinhenz 1998), which gives the impression of skin penetration without piercing the skin and can control for nonspecific cognitive factors known to confound acupuncture studies. Alternatively, sham (nearby non-acupoint) acupuncture can be used to control for physiological responses unrelated to acupoint specificity. Lastly, more appropriate paradigms such as the non-repeated event-related design paradigm should be implemented in future acupuncture studies (Cox and Savoy 2003). An appropriate paradigm in tandem with the implementation of data-driven analysis methods (free of any hypothesis about the temporal profile of acupuncture-related changes) will better inform the effects of acupuncture in the human brain.

This chapter briefly reviewed a variety of literature regarding the neurophysiological mechanisms of acupuncture and modern functional neuroimaging techniques useful for better understanding these mechanisms. Future studies evaluating the central and peripheral effects of needle stimulation in a well-controlled disease

model will assist the identification of which neurological substrates contribute to acupuncture's specific clinical effects. Concurrent physiological measurements (e.g., electrocardiography, pupillometry, and electrodermal activity) should also be adopted in conjunction with neuroimaging techniques to help correlate acupuncture-related neural responses with ANS functions. It is our hope that, as advancements in modern neuroimaging facilitate the further exploration of this ancient therapy, horizons will be broadened and the clinical implementation and utility of acupuncture will be enhanced.

## References

- Achard S, Bullmore E. Efficiency and cost of economical brain functional networks. *PLoS Comput Biol*. 2007;3(2):e17.
- Achard S, Salvador R, Whitcher B, et al. A resilient, low-frequency, small-world human brain functional network with highly connected association cortical hubs. *J Neurosci*. 2006;26(1):63–72.
- Albert R, Jeong H, Barabási AL. Error and attack tolerance of complex networks. *Nature*. 2000;406(6794):378–82.
- Bai L. The sustained effects of acupuncture. Doctoral dissertation, Xidian University; 2009c.
- Bai L, Qin W, Liang J, et al. Spatiotemporal modulation of central neural pathway underlying acupuncture action: a systematic review. *Curr Med Imaging Rev*. 2009a;5(3):167–73.
- Bai L, Qin W, Tian J. Time-varied characteristics of acupuncture effects in fMRI studies. *Hum Brain Mapp*. 2009b;30(11):3445–60.
- Baliki MN, Geha PY, Apkarian AV, et al. Beyond feeling: chronic pain hurts the brain, disrupting the default-mode network dynamics. *J Neurosci*. 2008;28(6):1398–403.
- Barabási A-L, Albert R. Emergence of scaling in random networks. *Science*. 1999;286(5439):509–12.
- Beijing S, Nanjing Colleges of Traditional Chinese Medicine. *Essentials of Chinese acupuncture*. Beijing: Foreign Language Press; 1980.
- Biella G, Sotgiu ML, Pellegata G, et al. Acupuncture produces central activations in pain regions. *NeuroImage*. 2001;14:60–6.
- Buchel C, Friston KJ. Modulation of connectivity in visual pathways by attention: cortical interactions evaluated with structural equation modeling and fMRI. *Cereb Cortex*. 1997;7(8):768–78.
- Buckner RL, Sepulcre J, Talukdar T, et al. Cortical hubs revealed by intrinsic functional connectivity: mapping, assessment of stability, and relation to Alzheimer's disease. *J Neurosci*. 2009;29(6):1860–73.
- Bullmore E, Sporns O. Complex brain networks: graph theoretical analysis of structural and functional systems. *Nat Rev Neurosci*. 2009;10(3):186–19.
- Casey KL. Forebrain mechanisms of nociception and pain: analysis through imaging. *Proc Natl Acad Sci U S A*. 1999;96:7668–74.
- Cho ZH, Chung SC, Jones JP, et al. New findings of the correlation between acupoints and corresponding brain cortices using functional MRI. *Proc Natl Acad Sci U S A*. 1998;95(5):2670–3.
- Clement JV, McLoughlin L, Tomlin S, et al. Increased beta-endorphin but not met-enkephalin levels in human cerebrospinal fluid after acupuncture for recurrent pain. *Lancet*. 1980;2(8201):946–9.
- Cox DD, Savoy RL. Functional magnetic resonance imaging (fMRI) “brain reading”: detecting and classifying distributed patterns of fMRI activity in human visual cortex. *NeuroImage*. 2003;19(2):261–70.
- Dai R, Han J, Shi X, et al. *Modern acupunctomics*: Zhejiang Science and Technology Publisher; 2013.
- Davis KD, Taylor SJ, Crawley AP, et al. Functional MRI of pain- and attention-related activations in the human cingulate cortex. *J Neurophysiol*. 1997;77:3370–80.

- Derbyshire SW, Jones AK, Gyulai F, et al. Pain processing during three levels of noxious stimulation produces differential patterns of central activity. *Pain*. 1997;73:431–45.
- Dhond RP, Witzel T, Yeh C et al. Spatiotemporal mapping the neural correlates of acupuncture. 13th Annual Organization for Human Brain Mapping Conference; 2007; Chicago.
- Dhond RP, Yeh C, Park K. Acupuncture modulates resting state connectivity in default and sensorimotor brain networks. *Pain*. 2008;136:407–18.
- Dodds PS, Muhamad R, Watts DJ. An experimental study of search in global social networks. *Science*. 2003;301(5634):827–9.
- Fair DA, Dosenbach NU, Church JA, et al. Development of distinct control networks through segregation and integration. *Proc Natl Acad Sci U S A*. 2007;104(33):13507–12.
- Fair DA, Cohen AL, Dosenbach NU, et al. The maturing architecture of the brain's default network. *Proc Natl Acad Sci U S A*. 2008;105(10):4028–32.
- Fair DA, Cohen AL, Power JD, et al. Functional brain networks develop from a “Local to Distributed” organization. *PLoS Comput Biol*. 2009;5(5):e1000381.
- Fields HL, Basbaum AI. Central nervous system mechanisms of pain modulation. In: Wall PD, Melzack R, editors. *Textbook of pain*. Edinburgh: Churchill Livingstone; 1999. p. 309–29.
- Fields HL, Heinricher MM, Mason P. Neurotransmitters in nociceptive modulatory circuits. *Annu Rev Neurosci*. 1991;14:219–45.
- Friston KJ. Functional and effective connectivity in neuroimaging: a synthesis. *Hum Brain Mapp*. 1994;2:56–78.
- Friston KJ, Frith CD, Fiddle PF, et al. Functional connectivity: the principal component analysis of large (PET) data sets. *J Cereb Blood Flow Metab*. 1993a;13(1):5–14.
- Friston KJ, Frith CD, Frackowiak RS. Time-dependent changes in effective connectivity measured with PET. *Hum Brain Mapp*. 1993b;1:69–80.
- Friston KJ, Jezzard P, Turner R. Analysis of functional MRI time-series. *Hum Brain Mapp*. 1994a;1:153–71.
- Gareus I, Lacour M, Schulte AC, et al. Is there a bold response of the visual cortex on stimulation of the vision-related acupoint GB 37? *J Magn Reson Imaging*. 2002;15(3):227–32.
- Guo HF, Tian J, Wang X, et al. Brain substrates activated by electroacupuncture (ea) of different frequencies (ii): role of fos/jun proteins in EA-induced transcription of preproenkephalin and preprodynorphin genes. *Brain Res Mol Brain Res*. 1996;43(1–2):167–73.
- Haker E, Egekvist H, Bjerring P. Effect of sensory stimulation (acupuncture) on sympathetic and parasympathetic activities in healthy subjects. *J Auton Nerv Syst*. 2000;79:52–9.
- Hampson M, Tokoglu F, Sun Z, et al. Connectivity–behavior analysis reveals that functional connectivity between left BA39 and Broca's area varies with reading ability. *NeuroImage*. 2006;31:513–9.
- Han JS. Acupuncture: neuropeptide release produced by electrical stimulation of different frequencies. *Trends Neurosci*. 2004;26:17–22.
- Haws CM, Williamson AM, Fields HL. Putative nociceptive modulatory neurons in the dorsolateral pontomesencephalic reticular formation. *Brain Res*. 1989;483:272–82.
- He Y, Chen Z, Evans A. Structural insights into aberrant topological patterns of large-scale cortical networks in Alzheimer's disease. *J Neurosci*. 2008;28(18):4756–66.
- Hellwig B. A quantitative analysis of the local connectivity between pyramidal neurons in layers 2/3 of the rat visual cortex. *Biol Cybern*. 2000;82(2):111–21.
- Hofbauer RK, Rainville P, Duncan GH, et al. Cortical representation of the sensory dimension of pain. *J Neurophysiol*. 2001;86:402–11.
- Hoffman GA, Harrington A, Fields HL. Pain and the placebo: what we have learned. *Perspect Biol Med*. 2005;48:248–65.
- Hsu CC, Weng CS, Sun MF, et al. Evaluation of scalp and auricular acupuncture on EEG, HRV, and PRV. *Am J Chin Med*. 2007;35:219–30.
- Hui KK, Liu J, Makris N. Acupuncture modulates the limbic system and subcortical gray structures of the human brain: evidence from fMRI studies in normal subjects. *Hum Brain Mapp*. 2000;9:13–25.

- Hui KK, Liu J, Marina O, et al. The integrated response of the human cerebro-cerebellar and limbic systems to acupuncture stimulation at ST 36 as evidenced by fMRI. *NeuroImage*. 2005;27:479–96.
- Jeanette E, Brian B, Victoria AH, et al. Is acupuncture effective for the treatment of chronic pain? A systematic review. *Pain*. 2000;86:217–25.
- Kamitani Y, Tong F. Decoding the visual and subjective contents of the human brain. *Nat Neurosci*. 2005;8(5):679–85.
- Kaptchuk TJ. Acupuncture: theory, efficacy, and practice. *Ann Intern Med*. 2002;136:374–83.
- Kong J, Ma L, Gollub RL, et al. A pilot study of functional magnetic resonance imaging of the brain during manual and electroacupuncture stimulation of acupuncture point (li-4 hegu) in normal subjects reveals differential brain activation between methods. *J Altern Complement Med*. 2002;8(7412):522–6.
- Kong J, Randy LG, Webb JM, et al. Test-retest study of fMRI signal change evoked by electroacupuncture stimulation. *NeuroImage*. 2007;34:1171–81.
- Kong J, Kaptchuk TJ, Webb JM, et al. Functional neuroanatomical investigation of vision-related acupuncture point specificity—a multisession fMRI study. *Hum Brain Mapp*. 2009;30(1):38–46.
- Korte C, Milgram S. Acquaintance networks between racial groups: application of small-world method. *J Pers Soc Psychol*. 1970;15(2):101–8.
- Kotter R. Neuroscience databases: tools for exploring brain structure-function relationships. *Philos Trans R Soc Lond Ser B Biol Sci*. 2001;356(1412):1111–20.
- Latora V, Marchiori M. Efficient behavior of small-world networks. *Phys Rev Lett*. 2001;87(19):198701.
- Latora V, Marchiori M. Economic small-world behavior in weighted networks. *Eur Phys J B*. 2003;32(2):249–63.
- Le BD, Villanueva L, Willer J. Diffuse noxious inhibitory controls (DNIC) in animals and man. *Acupunct Med*. 1991;9:47–56.
- Lindquist MA, Waugh C, Wager TD. Modeling state-related fMRI activity using change point theory. *NeuroImage*. 2007;35(3):1125–41.
- Liu WC, Feldman SC, Cook DB, et al. fMRI study of acupuncture-induced periaqueductal gray activity in humans. *Neuroreport*. 2004;15:1937–40.
- Liu Y, Liang M, Zhou Y, et al. Disrupted small-world networks in schizophrenia. *Brain*. 2008;131(4):945–61.
- Liu JX, Liang JM, Qin W, et al. Dysfunctional connectivity patterns in chronic heroin users: an fMRI study. *Neurosci Lett*. 2009;460(1):72–7.
- Liu J, Qin W, Guo Q. Distinct brain networks for time-varied characteristics of acupuncture. *Neurosci Lett*. 2010;468(3):353–8.
- Lowe MJ, Mock BJ, Sorenson JA. Functional connectivity in single and multislice echo-planar imaging using resting-state fluctuations. *NeuroImage*. 1998;7(2):119–32.
- MacPherson H, White A, Cummings M, et al. Standards for reporting interventions in controlled trials of acupuncture: the STRICTA recommendations. *J Altern Complement Med*. 2002;8(1):85–9.
- Mann F. Reinventing acupuncture: a new concept of ancient medicine. Great Britain: Biddles Ltd.; 1992.
- McKeown MJ, Makeig S, Brown GG, et al. Analysis of fMRI data by blind separation into independent spatial components. *Hum Brain Mapp*. 1998;6(3):160–88.
- McIntosh AR, Gonzalez-Lima F. Structural equation modeling and its application to network analysis in functional brain imaging. *Hum Brain Mapp*. 1994;2(1–2):2–22.
- Mechelli A, Price CJ, Noppeney U, et al. A dynamic causal modeling study on category effects: bottom-up or top-down mediation? *J Cogn Neurosci*. 2003;15(7):925–34.
- Milgram S. Small-world problem. *Psychol Today*. 1967;1(1):61–7.
- Millan MJ. Descending control of pain. *Prog Neurobiol*. 2002;66:355–474.
- Mitchell TM, Hutchinson R, Niculescu RS, et al. Learning to decode cognitive states from brain images. *Mach Learn*. 2004;57(1–2):145–75.
- Napadow V, Makris N, Liu J, et al. Effects of electroacupuncture versus manual acupuncture on the human brain as measured by fMRI. *Hum Brain Mapp*. 2005;24(3):193–205.



- Napadow V, Liu J, Li M, et al. Somatosensory cortical plasticity in carpal tunnel syndrome treated by acupuncture. *Hum Brain Mapp.* 2007;30:38–46.
- Napadow V, Dhond RP, Kim J, et al. Brain encoding of acupuncture sensation-coupling on-line rating with fMRI. *NeuroImage.* 2009a;47(3):1055–65.
- Napadow V, Dhond R, Park K, et al. Time-variant fMRI activity in the brainstem and higher structures in response to acupuncture. *NeuroImage.* 2009b;47(1):289–301.
- Newman ME. The structure and function of complex networks. *SIAM Rev.* 2003;45:167–256.
- Norman KA, Polyn SM, Detre GJ, et al. Beyond mind-reading: multi-voxel pattern analysis of functional magnetic resonance imaging data. *Trends Cogn Sci.* 2006;10(9):424–30.
- Oosterhof NN, Wiestler T, Downing PE, et al. A comparison of volume-based and surface-based multi-voxel pattern analysis. *Neuroimage.* 2011;56(2):593–600.
- Pariente J, White P, Frackowiak RS, et al. Expectancy and belief modulate the neuronal substrates of pain treated by acupuncture. *NeuroImage.* 2005;25(4):1161–7.
- Pastor-Satorras R, Vespignani A. Evolution and structure of the internet: a statistical physics approach. Cambridge: Cambridge University Press; 2004.
- Peets JM, Pomeranz B. CXBK mice deficient in opiate receptors show poor electroacupuncture analgesia. *Nature.* 1978;273:675–6.
- Pomeranz B. Acupuncture analgesia: basic research. In: Stux G, Hammerschlag R, editors. *Clinical acupuncture: scientific basis.* Berlin: Springer; 2001. p. 1–28.
- Porreca F, Ossipov MH, Gebhart GF. Chronic pain and medullary descending facilitation. *Trends Neurosci.* 2002;25:319–25.
- Price DD, Rafii A, Watkins LR. A psychophysical analysis of acupuncture analgesia. *Pain.* 1984;19:27–42.
- Qin W, Tian J, Bai L. fMRI connectivity analysis of acupuncture effects on an amygdala associated brain network. *Mol Pain.* 2008;4:55.
- Qin W, Bai L, Dai J. The temporal-spatial encoding of acupuncture effects in the brain. *Mol Pain.* 2011;7:19.
- Rainville P, Duncan GH, Price DD, et al. Pain affect encoded in human anterior cingulate but not somatosensory cortex. *Science.* 1997;277:968–71.
- Rainville P, Hofbauer RK, Paus T, et al. Cerebral mechanisms of hypnotic induction and suggestion. *J Cogn Neurosci.* 1999;11:110–25.
- Reijneveld JC, Ponten SC, Berendse HW, et al. The application of graph theoretical analysis to complex networks in the brain. *Clin Neurophysiol.* 2007;118(11):2317–31.
- Sakai S, Hori E, Umeno K, et al. Specific acupuncture sensation correlates with EEGs and autonomic changes in human subjects. *Auton Neurosci.* 2007;133:158–69.
- Salvador R, Suckling J, Coleman MR, et al. Neurophysiological architecture of functional magnetic resonance images of human brain. *Cereb Cortex.* 2005;15(9):1332–42.
- Siedentopf CM, Golaszewski SM, Mottaghy FM, et al. Functional magnetic resonance imaging detects activation of the visual association cortex during laser acupuncture of the foot in humans. *Neurosci Lett.* 2002;327(1):53–6.
- Smith SM, Beckmann CF, Ramnani N, et al. Variability in fMRI: a re-examination of inter-session differences. *Hum Brain Mapp.* 2005;24:248–57.
- Sporns O, Tononi G, Edelman GM. Theoretical neuroanatomy: relating anatomical and functional connectivity in graphs and cortical connection matrices. *Cereb Cortex.* 2000;10(2):127–41.
- Stanley HE. Introduction to phase transitions and critical phenomena. New York: Oxford University Press; 1971.
- Streitberger K, Kleinhenz J. Introducing a placebo needle into acupuncture research. *Lancet.* 1998;352:364–5.
- Supekar K, Menon V, Rubin D, et al. Network analysis of intrinsic functional brain connectivity in Alzheimer's disease. *PLoS Comput Biol.* 2008;4(6):e1000100.
- Takeda W, Wessel J. Acupuncture for the treatment of pain of osteoarthritic knees. *Arthritis Care Res.* 1994;7(3):118–22.



- Tortorici V, Vanegas H. Putative role of medullary off- and on-cells in the antinociception produced by dipyrone (metamizol) administered systemically or microinjected into PAG. *Pain*. 1994;57:197–205.
- Travers J, Milgram S. Experimental study of small-world problem. *Sociometry*. 1969;32(4):425–43.
- Urban MO, Gebhart GF. Supraspinal contributions to hyperalgesia. *Proc Nat Acad Sci U S A*. 1999;96:7687–92.
- van den Heuvel MP, Stam CJ, Boersma M, et al. Small-world and scale-free organization of voxel-based resting-state functional connectivity in the human brain. *NeuroImage*. 2008;43(3):528–39.
- Wager TD, Vazquez A, Hernandez L. Accounting for nonlinear BOLD effects in fMRI: parameter estimates and a model for prediction in rapid event-related studies. *NeuroImage*. 2005;25(1):206–18.
- Wang L, Zhu CZ, He Y, et al. Altered small-world brain functional networks in children with attention-deficit/hyperactivity disorder. *Hum Brain Mapp*. 2009;30(2):638–49.
- Wang L, Li Y, Metzack P, et al. Age-related changes in topological patterns of large-scale brain functional networks during memory encoding and recognition. *NeuroImage*. 2010;50(3):862–72.
- Watts DJ. *Small worlds: the dynamics of networks between order and randomness*. Princeton: Princeton University Press; 1999.
- Watts DJ, Strogatz SH. Collective dynamics of ‘small-world’ networks. *Nature*. 1998;393(6684):440–2.
- White A, Foster NE, Cummings M, et al. Acupuncture treatment for chronic knee pain: a systematic review. *Rheumatology*. 2007;46:384–90.
- Witt C, Brinkhaus B, Jena S, et al. Acupuncture in patients with osteoarthritis of the knee: a randomised trial. *Lancet*. 2005;366:136–43.
- Worsley KJ, Friston KJ. Analysis of fMRI time-series revisited again. *NeuroImage*. 1995;2(3):173–81.
- Wu MT, Hsieh JC, Xiong J, et al. Central nervous pathway for acupuncture stimulation: localization of processing with functional MR imaging of the brain—preliminary experience. *Radiology*. 1999;212:133–41.
- Wu MT, Sheen JM, Chuang KH, et al. Neuronal specificity of acupuncture response: a fMRI study with electroacupuncture. *NeuroImage*. 2002;16:1028–37.
- Xing GG, Liu FY, XX Q, et al. Long-term synaptic plasticity in the spinal dorsal horn and its modulation by electroacupuncture in rats with neuropathic pain. *J Pharmacol Exp Ther*. 2007;321:1046–53.
- Yan B, Li K, Xu J, et al. Acupoint-specific fMRI patterns in human brain. *Neurosci Lett*. 2005;383(3):236–40.
- Yoo SS, Teh EK, Blinder RA, et al. Modulation of cerebellar activities by acupuncture stimulation: evidence from fMRI study. *NeuroImage*. 2004;22:932–40.
- Zhang WT, Jin Z, Cui GH, et al. Relations between brain network activation and analgesic effect induced by low vs. high frequency electrical acupoint stimulation in different subjects: a functional magnetic resonance imaging study. *Brain Res*. 2003;982:168–78.
- Zhang Y, Qin W, Liu P, et al. An fMRI study of acupuncture using independent component analysis. *Neurosci Lett*. 2009;449(1):6–9.

Multi-Modality Neuroimaging Study on Neurobiological  
Mechanisms of Acupuncture

Liu, Z. (Ed.)

2018, V, 142 p. 56 illus., 47 illus. in color., Hardcover

ISBN: 978-981-10-4913-2